Journal of the Chinese Chemical Society, **1992**, *39*, 479-496

Some Recent Developments in NMR Approaches for Studying Liquid Molecular Dynamics and Their Biological Applications

William S. Price (卜威廉) and Lian-Pin Hwang* (黃良平)
Department of Chemistry, National Taiwan University, Taipei, Taiwan, R.O.C. and Institute of Atomic and Molecular Sciences, Academia Sinica, Taipei, Taiwan, R.O.C.

Two aspects of NMR relaxation are reviewed and their use in studying molecular dynamics in the liquid state and their application to biological systems are discussed. The first aspect concerns the use of 'null-point spectra' for observing the effects of higher rank multipoles (tensors) in the relaxation of quadrupolar nuclei. The second aspect concerns the effects of cross-correlation in homo- and heteronuclear spin systems. The application of null point spectral analysis to study cross-correlation in homonuclear spin systems is also discussed. Analysis of the effects of higher rank multipoles and of cross-correlation effects are shown to provide substantially more structural and motional information about spin systems than that available from traditional relaxation measurements. While similar in information content to multiple quantum techniques, the null point technique is experimentally less demanding. Over the past several years, work in this laboratory has been heavily involved in the theoretical formulation and the application of these techniques to biological systems. Illustrations of the use of these techniques to biological systems are drawn from our recent work.

INTRODUCTION

NMR has emerged to be one of the most powerful methods for investigating molecular dynamics in chemical and biochemical systems. Since NMR is a non-invasive technique it is particularly suited to the study of biological systems. Motion in biological systems covers a large range of timescales with small ions in solution having reorientational correlation times (τ_c) of the order of picoseconds whereas motion in lipid membranes can be in the order of nanoseconds to microseconds. In the simplest case the motion of small molecules is isotropic, however, normally molecules are not spherically symmetric and the motion has some degree of anisotropy. When the probe species is either bound to another molecule or simply part of a molecule the motion can be restricted or 'ordered'. Two common cases of ordered motion are methyl groups at the end of amino acid side chains and lipid molecules in biological membranes. The concept of ordering will be further discussed below. The molecular dynamics of small ions and molecules can be further complicated by binding and exchange to macromolecules and membranes.

Molecular dynamic studies have normally entailed the measurement and subsequent analysis of longitudinal (T_1), transverse (T_2) and spin-locked relaxation ($T_{1\rho}$) times of a probe species. These three relaxation times are sensitive to different motional frequencies. Depending on the experiment and the system being studied, the molecular dynamic parameters obtained generally consist of one (if the motion is isotropic) or more reorientational correlation times, bond lengths, angles and parameters characterizing interaction tensors. If the species studied is bound to a macromolecule it may be possible to infer details of the binding site from the relaxation data. The observed relaxation is normally some combination of relaxation mechanisms of both intra- and intermolecular origins and it is necessary to separate these contributions in order to determine molecular dynamic and structural parameters. The situation is somewhat easier in purely chemical rather than biological systems since there is more scope for altering the experimental conditions (e.g., solvent and temperature). Often the motion of the probe species is within the extreme narrowing limit (i.e., $\omega\tau_c << 1$; where ω is the Larmor frequency of the observed nucleus) and to a first approximation, the total observed relaxation is given by the sum of the relaxation rates of the relevant mechanisms. However, the individual relaxation mechanisms may cross-interact (also termed cross-correlation or interference) resulting in deviation from single exponential behavior (although the deviation may be too small to observe experimentally). If there is spin-spin coupling the individual resonances may exhibit differential longitudinal and differential transverse relaxation (differential line broadening; DLB). In the case of quadrupolar nuclei (i.e., nuclei with spin-quantum num-

This review is invited to commemorate the sixtieth anniversary of the Chinese Chemical Society.

ber, I, greater than 1/2) outside the extreme narrowing condition the observed relaxation is non-exponential.[1,2] Additionally, the resonance may appear asymmetric due to the presence of a dynamic frequency shift. However, in traditional relaxation measurements the relaxation data are generally well described by a single exponential and the observed lineshapes appear Lorentzian.

For both quadrupolar and non-quadrupolar nuclei the causes of deviation from exponential behavior provide a wealth of motional information complementary to that obtained through traditional analysis but the analysis is more difficult. The effects of cross-interactions in multispin systems have been recognized for a long time but it is only recently that the effect has been put to useful purposes instead of remaining as just a spectroscopic novelty. In the last several years there has been increasing interest and awareness of both the application and side effects of cross-interaction. The aim of this paper is to review some of the causes for non-exponential relaxation in both quadrupolar and non-quadrupolar systems, some methods for studying them and their advantages and applications to the study of molecular dynamics. In this paper we give some of the relevant theory for studying cross-correlation in multispin systems and of the use of multipole formulations for studying multiexponential relaxation in quadrupolar spin systems. To illustrate these methods, examples are drawn from some of our recent work: (1) using the null point method to study chloride ion binding to human serum albumin, (2) the application of differential line broadening caused by cross-interactions between different dipole-dipole (DD) pairs in methyl groups to study slow motion in macromolecules and macromolecular aggregates and (3) using the effects of cross-interaction between the dipole-dipole and chemical shift anisotropy (CSA) in the hypophosphite ion ($H_2PO_2^-$; HP) to measure the intracellular viscosity of human erythrocytes.

THE APPLICATION OF NULL POINT SPECTRA TO THE STUDY OF I = 3/2 QUADRUPOLAR SYSTEMS

Background

Quadrupolar nuclei play important roles in biological systems.[3] Well known examples of biologically important quadrupolar ions are $^{23}Na^+$(3/2), $^{39}K^+$(3/2), $^{25}Mg^{2+}$(5/2), $^{43}Ca^{2+}$(7/2), $^{35}Cl^-$(3/2) and $^{37}Cl^-$(3/2), where the number in parentheses represents the spin-quantum number, I. $^{27}Al^{3+}$(5/2) is transported by human serum transferrin and human serum albumin.[4] Recent work has shown that aluminium may be involved in Alzheimer's disease.[5] These ions commonly interact with biological macromolecules such as proteins in free solutions,[6,7] membrane bound proteins,[8,9] nucleic acids and polysaccharides. These ionic interactions have important biological roles such as enzyme activation, protein stabilization and roles in nerve and muscle function. Often the ions are in fast exchange between the binding site and free solution with the bound ion population being only a small fraction of the solution population. The slow motion at the bound site causes a significant effect on the overall ion relaxation even though the bound population is small. A number of reviews on the study of quadrupolar nuclei may be found in the literature.[10-13] It is well known that outside the extreme narrowing region, quadrupolar nuclei relax with I + 1/2 exponentials[1] and the relaxation is further complicated by exchange.[2,14] The extraction of multiple time constants from relaxation data is difficult.[8] In biological systems the quadrupolar nuclei are generally exchanging between sites with at least one of the binding sites being outside the extreme narrowing condition (e.g., a site attached to a membrane). Due to the difficulty in relaxation data analysis coupled with typically low sensitivity and broad resonances, very few studies of quadrupolar nuclei with I > 3/2 have been reported.[13,15,16] To circumvent these data analysis problems (experimentally demanding) multiple quantum experiments have been used, for example see refs. 16 to 19. However, we have demonstrated that the observation of the fine spectral structure near the 'null point' in inversion recovery experiments (see below) provides a less experimentally demanding method of studying I = 3/2 quadrupolar nuclei outside the extreme narrowing condition in a homogeneous system[20] and in an exchanging system where at least one of the sites is outside the extreme narrowing limit.[6,7] Null-point spectra were first observed for dipolar relaxation in methyl protons (in which the quartet of spin levels is formally equivalent to an isolated I = 3/2 nucleus) by Haslinger and co-workers.[21-24] Subsequently this effect was analyzed in terms of cross-dipolar interactions by Lee and Hwang.[25] Null point spectra for quadrupolar nuclei undergoing chemical exchange were first found experimentally by Urry and co-workers.[26,27]

A number of mathematical formalisms have been applied to study the relaxation of quadrupolar nuclei. However the use of state multipoles[28] (statistical tensors) has become popular since the multipole operators transform very simply under rotations and can be associated with measurable spectral magnetizations.[29,30] State multipoles are specific linear combinations of the normal density matrix elements. The following discussion is relevant to I = 3/2 quadrupolar nuclei, although the theory can be generalized

to nuclei of any spin quantum number. A rank k state multipole with tensorial component m is defined by,

$$\sigma_m^k \equiv \sum_\alpha \sum_{\alpha'} \rho_{\alpha\alpha'}(-1)^{I-\alpha}\sqrt{2k+1}\begin{pmatrix} I & I & k \\ \alpha & -\alpha' & -m \end{pmatrix}, \quad (1)$$

where $\rho_{\alpha\alpha'}$ are density matrix elements and $\begin{pmatrix} I & I & k \\ \alpha & -\alpha' & -m \end{pmatrix}$ is a 3-j symbol.[31,32] σ_m^k corresponds to k-quantum coherence for m = 1 or -1; for a multi-spin system it corresponds to k-spin order for m = 0, σ_0^1 corresponds to longitudinal magnetizations and σ_1^1 (or σ_{-1}^1) corresponds to transverse magnetizations. State multipoles transform as a component of the full rotation group, for example, an on resonance radio frequency (rf) pulse transforms the state multipole components according to the relation,[20,33]

$$(\sigma^+)_m^k = \sum_n D_{mn}^k(\phi - \pi/2, \theta, \pi/2 - \phi)(\sigma^-)_n^k \quad (2)$$

where $D_{mn}^k(\alpha,\beta,\gamma)$ is a Wigner rotation matrix element,[31,32] θ is the rf pulse angle, ϕ is the rf phase angle associated with the θ angle pulse with respect to the x axis in the rotating frame and the superscript +/- indicate the state multipoles after/before the pulse.

The fine structure in the null point is a consequence of the evolution of the rank 3 multipole. The maximum value of the rank 3 multipole and the minimum absolute amplitude of the rank 1 multipole occur at approximately the same time as the null point in the inversion recovery experiment (See Fig. 1). The asymmetry in the null point results from the dynamic frequency shift[6,20] and this frequency shift becomes apparent only when the extreme narrowing condition fails (see for example, Fig. 2 of ref. 20). Eliav and co-workers[19] have recently proposed that the formation of even rank tensors may serve as a general method for the detection of order in biological systems due to motionally non-averaged quadrupolar interactions.

An Example: Chloride Binding to Human Serum Albumin

Human serum albumin (HSA), with a molecular weight of 66439, is the most abundant protein in blood plasma. It plays an important role in the transport of endogenous and exogenous species. Chloride ions binding to HSA form a three-site system with the chloride ions exchanging rapidly on the NMR timescale between the free solution sites (f), a weak (w) and a strong class (s) of binding site on the protein surface. Exchange between the s and w sites is neglected since it is very slow and is limited by the Cl^- diffusion rate on the protein surface. Both the s and w sites are outside the extreme narrowing condition. In the presence of sodium dodecyl sulfate (SDS) the system reduces to a two site-system with the SDS blocking the strong class of binding sites. The system is depicted schematically in Fig. 2. The Hamiltonian for the quadrupolar interaction may be written as,[34,35]

$$\mathcal{H}_Q(t) = \frac{eQ}{2I(2I-1)\hbar}\sum_{m=-2}^{2}(-1)^m A_{-m}V_m(t) \quad (3)$$

where $\hbar$ is Planck's constant divided by 2π, eQ is the electric quadrupole moment of the nucleus, the A_m are second rank irreducible spin tensor operators and the V_m are components of the second rank irreducible electric field gradient tensor. We use the definitions of Halle and Wennerström[36] for A_m and V_m. The spin-operators are evaluated in the laboratory frame (L) whereas the field gradient components are expressed in the principal axes system (F) fixed at the nucleus.

Redfield theory is then used to account for the time evolution of the state multipoles.[37,38] In the case of a

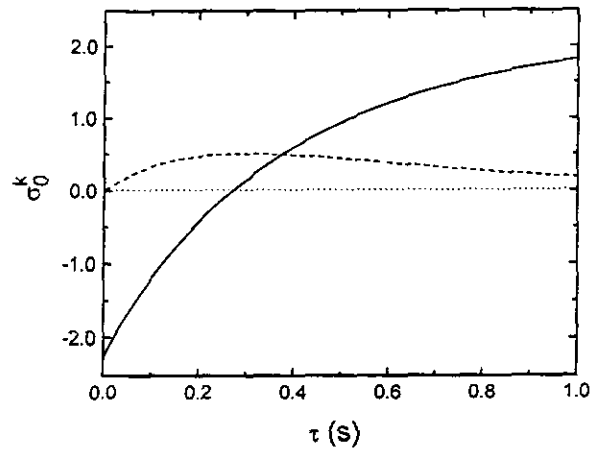

Fig. 1. The time evolution of the rank 1 (σ_0^1, —) and rank 3 (σ_0^3, -----) longitudinal state multipoles. The plot shows that the maximum value of the rank 3 multipole occurs at approximately the same time as the minimum absolute signal amplitude in the inversion recovery experiment. The ordinate is in units of $\gamma_1\hbar B_0/(2I+1)$ kT. The evolution of the state multipoles was calculated using a quadrupolar coupling constant of 42.7 kHz, a spectrometer frequency of 116.6 MHz (i.e., ^{7}Li at 7.05 T) and a reorientational correlation time of the electric field gradient at the nucleus of 1.13 ns.

homogeneous system the rate equations for longitudinal and transverse relaxation take the form,[20] respectively,

$$\frac{d}{dt}\begin{bmatrix}\sigma_0^1\\ \sigma_0^3\end{bmatrix} = -R\begin{bmatrix}\sigma_0^1\\ \sigma_0^3\end{bmatrix} \quad (4a)$$

$$\frac{d}{dt}\begin{bmatrix}\sigma_1^1\\ \sigma_1^3\end{bmatrix} = [-R' - i\omega I]\begin{bmatrix}\sigma_1^1\\ \sigma_1^3\end{bmatrix} \quad (4b)$$

where **I** is a unit matrix and **R** and **R'** are the relaxation matrices for the longitudinal and transverse components of the multipoles, respectively. The relaxation matrices are defined in Ref. 20. However, for two-site exchange the rate equations for longitudinal and transverse relaxation are given by,[6] respectively,

$$\frac{d}{dt}\begin{bmatrix}\rho_f\\ \rho_w\end{bmatrix} = \begin{bmatrix}-R_f - k_{fw}I & k_{wf}I\\ k_{fw}I & -R_w - k_{wf}I\end{bmatrix}\begin{bmatrix}\rho_f\\ \rho_w\end{bmatrix} \quad (5a)$$

$$\frac{d}{dt}\begin{bmatrix}\rho_f'\\ \rho_w'\end{bmatrix} = \begin{bmatrix}-R_f' - k_{fw}I - i(\omega-\delta_f)I & k_{wf}I\\ k_{fw}I & -R_w' - k_{wf}I - i(\omega-\delta_w)I\end{bmatrix}\begin{bmatrix}\rho_f'\\ \rho_w'\end{bmatrix} \quad (5b)$$

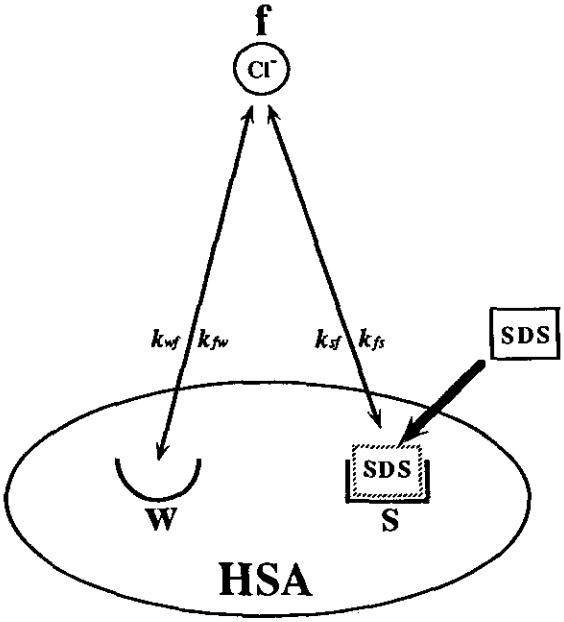

Fig. 2. Schematic representation of chloride ion binding to HSA. The exchange of chloride ions between the free (f) and weak (w) sites occurs independently of the exchange between the free and strong (s) sites. Direct exchange between sites s and w is neglected as it would be very slow as it is limited by the Cl- ion diffusion rate on the HSA surface. There are n_s and n_w strong and weak chloride binding sites per HSA molecule. The population of chloride ions at the free, strong and weak sites is denoted by p_f, p_s, and p_w, respectively. k_{xy} are the microscopic rate constant for transfer from site x to site y (where x,y = f,s,w). The chloride ion binding to the strong site may be inhibited by stoichiometric amounts (with respect to the number of strong binding sites) of SDS.

where k_{fw} is the microscopic rate constant for transfer from site f to site w and k_{wf} is the microscopic rate constant for transfer from site w to site f. $\mathbf{R}_f$ (or $\mathbf{R}_w$) is the Redfield relaxation matrix for the longitudinal components in the state multipole representation in sites f (or w). $\mathbf{R}_f'$ (or $\mathbf{R}_w'$) is the Redfield relaxation matrix for the transverse components in the state multipoles in sites f (or w). This matrix may be directly derived from the transformation from the Redfield relaxation matrix in accordance with the interaction Hamiltonian (i.e., Eq. (3)). The column density matrices ρ_f, ρ_w, ρ_f' and ρ_w' are defined as column density matrices of state multipoles in sites f and w, respectively, by

$$\tilde{\rho}_f \equiv [(\sigma_0^1)_f, (\sigma_0^3)_f], \quad \tilde{\rho}_w \equiv [(\sigma_0^1)_w, (\sigma_0^3)_w],$$
$$\tilde{\rho}_f' \equiv [(\sigma_1^1)_f, (\sigma_1^3)_f] \quad \text{and} \quad \tilde{\rho}_w' \equiv [(\sigma_1^1)_w, (\sigma_1^3)_w].$$

To guarantee the validity of Eq. (5) the condition $\tau_{exw} >> \tau_w$ must holds, where τ_w is the fluctuation correlation time of the electric field gradient at the weak-site and we define

$$\tau_{exw} = \frac{p_w}{k_{fw}} = \frac{p_f}{k_{wf}} \quad (6)$$

where p_f and p_w are the chloride ion populations at the free and weak sites, respectively. Also in the fast exchange limit the condition $|\delta_f - \delta_w|\,\tau_{exw} << 1$ hold, where δ_f and δ_w are the chemical shifts in angular frequency units of the free and weak sites. We can then modify Eq. (5) to encompass simple three-site exchange where the exchange between sites s and f occur independently of the exchange between sites s and w. The density matrix equations for longitudinal and transverse relaxation including exchange between the free, strong and weak sites is described by the rate equations, respectively, by

$$\frac{d}{dt}\begin{bmatrix}\rho_f\\ \rho_s\\ \rho_w\end{bmatrix} = \begin{bmatrix} -R_f - (k_{fs}+k_{fw})I & k_{sf}I & k_{wf}I \\ k_{fs}I & -R_s - k_{sf}I & 0 \\ k_{fw}I & 0 & -R_w - k_{wf}I \end{bmatrix}\begin{bmatrix}\rho_f\\ \rho_s\\ \rho_w\end{bmatrix} \quad (7a)$$

and

$$\frac{d}{dt}\begin{bmatrix}\rho'_f\\ \rho'_s\\ \rho'_w\end{bmatrix} = \begin{bmatrix} -R'_f - (k_{fs}+k_{fw})I - i(\omega-\delta_f)I & k_{sf}I & k_{wf}I \\ k_{fs}I & -R'_s - k_{sf}I - i(\omega-\delta_s)I & 0 \\ k_{fw}I & 0 & -R'_w - k_{wf}I - i(\omega-\delta_w)I \end{bmatrix}\begin{bmatrix}\rho'_f\\ \rho'_s\\ \rho'_w\end{bmatrix} \quad (7b)$$

where

$$\tilde{\rho}_f \equiv [(\sigma_0^1)_f, (\sigma_0^3)_f], \quad \tilde{\rho}_s \equiv [(\sigma_0^1)_s, (\sigma_0^3)_s],$$
$$\tilde{\rho}_w \equiv [(\sigma_0^1)_w, (\sigma_0^3)_w], \tilde{\rho}'_f \equiv [(\sigma_1^1)_f, (\sigma_1^3)_f],$$
$$\tilde{\rho}'_s \equiv [(\sigma_1^1)_s, (\sigma_1^3)_s] \quad \text{and} \quad \tilde{\rho}'_w \equiv [(\sigma_1^1)_w, (\sigma_1^3)_w].$$

To guarantee the validity of Eq. (7) the conditions $\tau_{exs} >> \tau_{ss}$ and $\tau_{exw} >> \tau_w$ must hold, where τ_{exs} is defined by,

$$\tau_{exs} = \frac{p_s}{k_{fs}} = \frac{p_f}{k_{sf}} \quad (8)$$

where p_s, is the population of chloride ions at the strong binding sites. Also in the fast exchange limit the condition $|\delta_f - \delta_s|\ \tau_{exs} << 1$ holds, where δ_s is the chemical shift in angular frequency units of the strong sites.

Experimental null point spectra of chloride binding to HSA in the presence and absence of SDS are shown in Figs. 3 and 4, respectively. The corresponding null point simulations are also given in the figures. The null point spectra were simulated using a complete formulation of the relaxation processes (i.e., both longitudinal and transverse), chemical exchange and the effects of the rf pulses occurring throughout the inversion-recovery pulse sequence and the subsequent acquisition period (i.e., π-τ-π/2-Acq.). The equilibrium state multipoles, calculated from the corresponding density matrix elements using Eq. (1) are $(\sigma_0^1)_{eq} = \sqrt{5\gamma}hB_0/(2I+1)kT$ and $(\sigma_0^3)_{eq} = 0$, where k is the Boltzmann constant, T is temperature and B_0 is the strength of the static magnetic field. The multipoles are then multiplied by the appropriate population weighting factors. The effect of the π pulse is calculated using Eq. (2) and immediately after the pulse the state multipoles are given by $(\sigma_0^k)_{f(w)} = -p_{f(w)}(\sigma_0^k)_{eq}$, where $(\sigma_0^k)_{eq}$ is the equilibrium state multipole. Then Eq. (5a) is used to follow the evolution of the longitudinal magnetization and the effects of chemical exchange during the delay time, τ. The effects of the π/2 pulse are calculated using Eq. (2) and the result forms the initial condition for calculating the transverse magnetization evolution and the effects of exchange during the acquisition period using Eq. (5b). The π/2 pulse transforms the longitudinal state multipoles into transverse state multipoles. The rf pulses are considered to be delta functions and so do not cause mixing of the multipoles of the w site and of the f site. The spectral lineshape is related to the real part of the Fourier-Laplace transform of the $((\sigma_1^1)_f + (\sigma_1^1)_w)$ term (which corresponds to the free induction

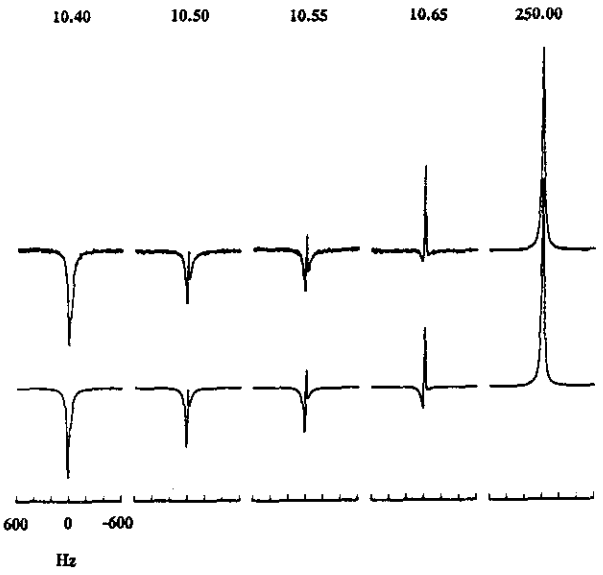

Fig. 3. Experimental (top) and simulated (bottom) ^{35}Cl inversion-recovery spectra as a function of the τ delay time at 310 K of a sample containing HSA (0.45 mM), Cl^- (1 M) and sufficient SDS to inhibit Cl^- binding to the strong binding sites at pH 7.4. The null point spectra were measured at 29.4 MHz.

decay), which evolves during the acquisition period. The null point spectra being those spectra acquired with τ values such that the net magnetization is near zero.

While the binding at the weak site was well described by a single correlation time, a single correlation time was insufficient for simulating the relaxation at the strong site. In particular the 'shoulders' of the null point spectra could not be properly simulated. The effects of order on the chloride binding at the strong sites are clearly shown by comparing the difference in the 'shoulders' of the null point spectra in Figs. 3 and 4 (N.B. the different abscissal scales). To avoid over-interpretation of the relaxation data involving the strong site we used a modification of the two-step model free approach[36] to describe the internal motion. This model required a slow;correlation time, τ_{ss}, a fast correlation time, τ_{sf}, and an order parameter, A. τ_{ss} represents an apparent reorientational correlation time for the overall motion of HSA whilst τ_{sf} is a correlation time representing the fast internal motion at the strong binding sites. In our modification we have omitted Halle and Wennerström's molecular frame since we are dealing with an atomic system while their system was molecular (i.e., water). In our model, the director system (D) was introduced with its z axis perpendicular to the protein surface. Transformation between the three frames was accomplished using second rank Wigner rotation matrices,[31,32]

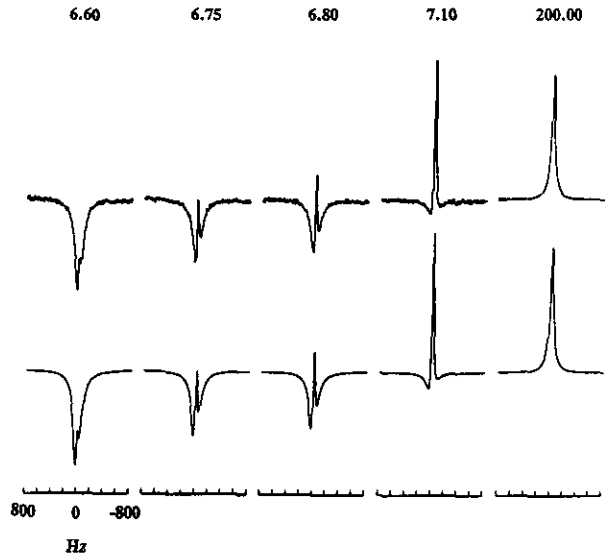

Fig. 4. Experimental (top) and simulated (bottom) ^{35}Cl inversion-recovery spectra as a function of the τ delay time at 310 K of a sample containing HSA (0.45 mM) and Cl^- (1 M) in the absence of SDS at pH 7.4. The null point spectra were measured at 29.4 MHz.

$$V_m^L(t) = \sum_{m'}\sum_{m''} D_{m''m'}[\Omega_{FD}(t)]D_{m'm}[\Omega_{DL}(t)]V_{m''}^F \quad (9)$$

where $\Omega_{FD}(t)$ and $\Omega_{DL}(t)$ are the time-dependent Euler angles. The main feature of the two-step model is that the motions giving rise to the time dependence in $\Omega_{LD}(t)$ and $\Omega_{DF}(t)$ occur on such different time scales that Ω_{LD} and Ω_{DF} are statistically independent. The order parameter, A, is defined by

$$A \equiv (V_0^F)^{-1}\sum_m \langle D_{0m}^2(\Omega_{DF})\rangle_{DF} V_m^F \quad (10)$$

where $\langle\rangle_{DF}$ denotes averaging over Ω_{DF}. Thus A is confined to the range [-1, 1] and A = 0 for isotropic motion. The order parameter-characterizes the average fluctuations of the electric field gradient about the director axis.

If we assume that the reorientational diffusion of the protein molecule is isotropic then, using the Wigner-Eckart theorem,[31,32] the time correlation function of the irreducible tensorial component of the electric field gradient, G(t), may be expressed in terms of the time correlation function of its zeroth component in the L frame as,

$$G(t) \equiv \langle V_0^{L*}(0)V_0^L(t)\rangle \quad (11)$$

$V_0^L(t)$ can be separated into parts with slow and fast time dependence. There are no cross-correlations since we have assumed statistical independence of the fast and slow motions and so G(t) may be expressed as

$$G(t) = G(t)_f + G(t)_s \quad (12)$$

where

$$G(t)_s = \frac{1}{5}(AV_0^F)^2 e^{-\frac{t}{\tau_{ss}}} \quad (13)$$

and

$$G(t)_f = \frac{1}{5}(V_0^F)\left[1 + \frac{1}{3}\eta^2 - A^2\right]e^{-\frac{t}{\tau_{sf}}} \quad (14)$$

where

$$V_0^F = \frac{\sqrt{6}}{2}eq. \quad (15)$$

In the above equations η is the asymmetry parameter and

eq is the electric field gradient at the nucleus at the bound site. In using the two-step model the same longitudinal and transverse relaxation matrices are used as given in our previous publication[20] except that the spectral density functions are now defined by,

$$J_n \equiv \int_0^\infty G(t)\cos(n\omega t)dt = \frac{3}{10}(eq)^2\left[\left(1+\frac{\eta^2}{3}-A^2\right)J_{nf}+A^2J_{ns}\right] \quad (16)$$

and

$$Q_n \equiv \int_0^\infty G(t)\sin(n\omega t)dt = \frac{3}{10}(eq)^2\left[\left(1+\frac{\eta^2}{3}-A^2\right)Q_{nf}+A^2Q_{ns}\right], \quad (17)$$

where

$$J_{nf}=\frac{\tau_{sf}}{1+(n\omega\tau_{sf})^2}, \quad J_{ns}=\frac{\tau_{ss}}{1+(n\omega\tau_{ss})^2},$$

$$Q_{nf}=\frac{n\omega\tau_{sf}^2}{1+(n\omega\tau_{sf})^2} \text{ and } Q_{ns}=\frac{n\omega\tau_{ss}^2}{1+(n\omega\tau_{ss})^2}.$$

If A is set to 0 then the definitions given for J_n and Q_n agree with those given in our previous work.[20]

The fitting procedure for the three-site exchange was similar to that for two-site exchange except that the initial condition after the π pulse now involves population weighting of sites f, s and w and with the assumption that the rf pulses do not cause mixing between the multipoles of sites f, s and w. Also, Eq. (9) is substituted for Eq. (7) and Eq. (10) is substituted for Eq. (8) and the spectral lineshape is now related to the real part of the Fourier-Laplace transform of the $((\sigma_1^1)_f + (\sigma_1^1)_s) + (\sigma_1^1)_w)$ term, which evolves during the acquisition period. Further details on the choice of fitting parameters may be found elsewhere.[7]

The number of strong binding sites per HSA molecule, n_s, was determined from an SDS titration, but we were unable to determine the number of weak binding sites, n_w, per molecule. From simulating the null point spectra acquired in the presence of SDS at 310 K an upper bound for p_w was determined to be 0.024. The bound population occurs in the relaxation equations as a product of the square of the quadrupolar coupling constant for the weak binding sites, χ_w (i.e., $\chi_w = e^2Qq/h$; where h is the Planck constant). Since the bound population could not be determined the quadrupolar coupling constant for the weak site could only be determined as $p_w\chi_w^2 = 6260$ kHz^2 together with a correlation time of $\tau_w = 3.4$ ns. A number of sets of parameters for the strong sites were found that were consistent with the longitudinal and transverse relaxation times. However, only a much smaller group of these were able to fit the obseNed null point spectra obtained in the absence of SDS. The dynamic frequency shift of the null point was found to be almost totally dependent on the value of τ_{ss} and hence providing a means for determining τ_{ss}. For the strong sites the null point spectra were analyzed to give $p_s\chi_s^2(1 + \eta^2/3 - A^2)\tau_{sf} = 278$ rad s^{-1} (χ_s is the quadrupolar coupling constant for the strong binding sites), $p_s\chi_s^2A^2\tau_{ss} = 4710$ rad s^{-1}, $\tau_{ss} = 35$ ns and an upper bound value of τ_{sf} of 0.50 ns.

The value determined for τ_{ss} is in good agreement with values determined for the overall reorientational correlation time of HSA using Debye theory and from dielectric measurements. Similarly the upper bound value of τ_{sf} obtained is consistent with the notion of the chloride ion being bound to a rapidly moving side chain.

EFFECTS OF CROSS-INTERACTION IN MULTISPIN SYSTEMS

Background

Cross-correlations arise when the fluctuations of different interactions of the same tensorial rank and spatial transformation properties are partly correlated as a result of molecular tumbling. In the course of relaxation and in the absence of rf irradiation, cross-correlation between different relaxation mechanism leads to the partial conversion of Zeeman polarization into higher rank coherences and spin order. Thus the appearance of terms of higher rank may be deemed to be the characteristic signature of cross-correlation. For example in an AX_2 spin system cross-correlation may lead to creation of longitudinal two-spin ($<2I_zS_z>$) and three-spin order ($<I_zS_z'S_z''>$); where the I represents the A spin and S' and S'' represent the X spins. Krishnan and Kumar[39] have shown in their analysis of an ABX spin system that while in the weak coupling limit, cross-correlations appear only in single quantum transition probabilities and decrease in magnitude as $\omega\tau_c$ increases, but in the strong coupling limit the states are mixed and the cross-correlations affect zero and double quantum t-Mnsitions as well. Cross-correlation should not be confused with normal cross-relaxation (Overhauser effects) which lead only to the interconversion of single-spin terms (e.g., $<S_z> \rightarrow <I_z>$). The main interactions considered so far are the dipole-dipole and chemical shift anisotropy, although other cross-interactions have been obseNed such as dipolar-quadrupolar.[40] There have been a number of

review articles dealing with cross-correlation in both heteronuclear and homonuclear spin systems.[41-45] Experimentally the effects of cross-correlation result in non-exponential longitudinal and/or transverse relaxation. In coupled systems differential longitudinal and/or differential transverse relaxation (i.e., differential line broadening) will be evident.

The synergistic nature of the cross-interaction can be exploited to quantify the contributing relaxation mechanisms obviating the need for Overhauser or magnetic field dependence studies.[42-55] Specifically, CSA-DD cross-interactions can be used to detemmine: (1) the absolute sign of the indirect coupling constant;[54,56,57] (2) details of the CSA tensor (σ; not to be confused with the state multipoles mentioned above) including, the symmetry of the tensor, the magnitude of the anisotropy (i.e., $\Delta\sigma$) and the orientation with respect to the molecular axis;[52-54,58,59] and (3) providing that the principal axis of the chemical-shift tensor is neither parallel nor at the magic angle with the AX internuclear vector, the motional anisotropy.[60] DD-DD cross-interactions can provide information on internuclear distances and the angles subtended by internuclear vectors.[39,61,62] Two-dimensional longitudinal two-spin order spectroscopy has been used to obtain NMR finger prints for proteins.[63] Recently measurements of cross-interaction between NH groups in proteins have been used in conjunction with traditional relaxation measurements to map the spectal densities of the NH motions in the proteins.[64] Of particular importance to molecular dynamic studies in biological studies, where there is little scope for altering the solvent, cross-interaction studies allow the separation of intramolecular and intermolecular (i.e., random field) contributions to the relaxation mechanism. This separation allows more accurate estimate of the reorientational correlation time to be obtained.[55] Farrar and Jablonsky[65] have shown that the random field terms provide information about the motion of the solvent molecules hydrogen bonded to the observed species.

In theory one could study the effects of cross-correlation by analyzing the multi-exponential relaxation data, however, the time constants are generally too similar to permit analysis.[66] Double and triple-quantum and selective ("soft-NOESY") exchange spectroscopy has also been used to monitor two- and three-spin order in homonuclear systems.[62,67-69] The creation of three-spin longitudinal order ($4I_{kz}I_{lz}I_{mz}$) in the NOESY experiment is direct evidence for cross-correlations between dipolar vectors. More recently we have used null point spectral analysis to study cross-correlation (or three-spin order) in methyl groups (an A_3 spin system). Similarly to the quadrupolar nuclei, asymmetry due to the dynamic frequency shift is noted in the fine spectral structure at the null point. Werbelow[70] and Thevand and Werbelow[71] have discussed the effects of the dynamic frequency shift in the null point spectra of methyl groups. The dynamic frequency shift can be used to differentiate between multispin order induced by cross-correlation and from multispin order resulting from the failure of extreme narrowing.[71] In heteronuclear spin systems selective excitation has been used to study cross-correlation[48-55] and recently a heteronuclear version of the soft-NOESY experiment has also been used.[72] The conversion of Zeeman order into two- and three-spin order depends on cross-correlation spectral densities at the Larmor frequency, these spectral densities cancel within the extreme narrowing limit and consequently two- and three-spin order cannot arise through relaxation in macromolecules.[73] However, if the motion is too slow the second order perturbation theory does not hold and so Redfield theory cannot be used and other approaches such as the stochastic Liouville equation (SLE; see below) must be used. Following a suggestion by Bull[74], cross-correlation has been studied in the rotating frame and thereby removing the restriction of being in the extreme narrowing condition.[61,73]

DLB was first observed and explained in electron spin resonance.[75] Such effects have been observed in ^{19}F-^{1}H,[76] ^{31}P-^{19}F,[46,77] ^{15}N-^{1}H,[78-80] ^{31}P-^{1}H,[81] ^{1}H-^{1}H,[82] ^{13}C-^{1}H,[57,83] and ^{13}C-^{2}H systems.[48] DLB is likely to be significant when at least one of the correlation times is not within the extreme narrowing condition and when at least two of the relaxation mechanisms are of comparable magnitudes. DLB has a number of applications in both the liquid[84-86] and solid state[66,87-89]. Recently the number of applications of DLB in the literature has been growing, including methyl groups in surfactant systems,[49,50] methyl ^{13}C-enriched transfer RNA,[90] elastomeric (polymers) and liquid crystals.[89] In the solid state DLB has been used to probe membrane structure[88] and the gel-phase of a cationic surfactant/polyanion system.[91] In the study of the structure and dynamics of macromolecules and molecular aggregates DLB is proving to be a very valuable technique since, different to standard relaxation measurements, it allows measurements of spectral densities in the low frequency region (e.g., $\tau_c > 10^{-8}$ s).[50]

It is important to understand the effects of cross-correlation not only for their own sake but also because cross-correlation effects can cause side effects in other experiments. Cross-correlation can cause anomalous peaks in 2D correlation (COSY) experiments and multiple quantum filtered experiments of large molecules.[92-99] For example AX_3 systems, which commonly occur in amino acids, according to coherence selection rules[100,101] should not give

cross-peaks in four-quantum filtered COSY spectra. However, in the case of slowly tumbling macromolecules where the transverse relaxation is multiexponential, these coherence transfer rules do not hold and "forbidden" cross peaks are observed. Similar effects can be found for I = 3/2 quadrupolar nuclei.[102] Cross-correlation can also cause relaxation-allowed coherence transfer between spins which are not scalar coupled to each other.[96] If cross-correlation effects are not accounted for when analyzing cross-relaxation measurements (i.e., nuclear Overhauser effect; NOE) the distances determined between nuclei may be incorrect.[39,68,69,103-106] For aromatic protons the CSA-DD cross-correlations can be even larger than the Overhauser effect.[69,107] Kay and Torchia[106] evaluated the effects of cross-correlation on ^{13}C T_1 and T_2 and NOE measurements of methyl protons attached to a macromolecule. They found large effects on the T_2 measurements but smaller effects on T_1 and NOE measurements. Bull[67] has shown that the neglect of cross-interaction terms can only be justified in NOESY experiments in the case of short mixing times. As these interference terms may complicate the obseNed relaxation, some groups have made efforts to develop pulse sequences to remove them.[108-109] Irradiation of spins directly attached to the heteronuclei eliminates the effects of cross-correlation on the observed heteronuclear spin-lattice relaxation rate constants.[10]

Example 1: The Application of Differential Line Broadening in Proton-Coupled ^{13}C Spectra to Determine the Molecular Dynamics of Methyl Groups in a Viscoelastic Micellar System

The methyl group is very common in lipids, proteins, macrocyclic ion carriers, antibiotics and macromolecules in general. The methyl groups in such molecules normally do not undergo isotropic motion but are instead restricted to rotation in a cone about the methyl C_3 axis, although this could be further restricted by steric constraints. The motion is further complicated by the method of linkage back to the macromolecule (e.g., the length of the amino acid side-chain). Thus, the ^{13}C NMR relaxation of a methyl group contains contributions from the overall reorientation of the molecule and also from the internal rotation of the methyl group.[111-113] In the present example we examine the relaxation of the *N*-methyl group of hexadecyltrimethylammonium bromide (CTAB) and sodium salicylate (Nasal) in water. This system becomes viscoelastic when CTAB and Nasal are mixed in equimolar ratios at concentrations of about 13 mM. A proton-coupled ^{13}C spectrum of the *N*-methyl group of CTAB at 52 °C is given in Fig. 5. The CSA interaction and DD interaction with the protons dominate the methyl ^{13}C relaxation. The Hamiltonian for the system is given by

$$\mathcal{H} \equiv \mathcal{H}_Z + \mathcal{H} \equiv \mathcal{H}_Z + \mathcal{H}_{CSA} + \mathcal{H}_{DD} \tag{18}$$

where the Zeeman Hamiltonian is defined by,

$$\mathcal{H}_Z = -\omega_C I_Z - \omega_H S_Z + J_{CH} I_Z S_Z \tag{19}$$

which includes the Zeeman terms for ^{13}C (I spins) and ^1H (S spin) as well as the first order correction for the spin-spin coupling between them. J_{CH} (Hz) is the spin-spin coupling constant. The CSA Hamiltonian is defined by,[35]

$$\mathcal{H}_{CSA} = FD^{(2)}_{0,0}(\Omega)I_Z - \left(\frac{3}{8}\right)^{1/2} F\{-D^{(2)}_{0,1}(\Omega)I_+ + D^{(2)}_{0,-1}(\Omega)I_-\} \tag{20}$$

where $F = 2/3(\sigma_{||} - \sigma_\perp)\omega_I$ in which $\sigma_{||}$ and $\sigma_\perp$ are the parallel and perpendicular values of the CSA tensor and n represents the Euler angles relating one axis system to another. The dipolar Hamiltonian depends on Ω and the internal rotation coordinates $(\alpha, \beta, 0)$. α is the rotating angle of the methyl group, β is the fixed angle between the methyl C_3 axis and the C-H direction. The dipolar Hamiltonian may be written as the scalar product of two tensors,[35,114]

$$\mathcal{H}_{DD}(\Omega,\alpha) = \sum_{p,q} D^{(2)}_{q,0}(\alpha,\beta,0)D^{(2)}_{q,p}(\Omega)A_p = \sum_{p,q} \exp(iq\alpha)d^{(2)}_{q,0}(\beta)D^{(2)}_{q,p}(\Omega)A_p \tag{21}$$

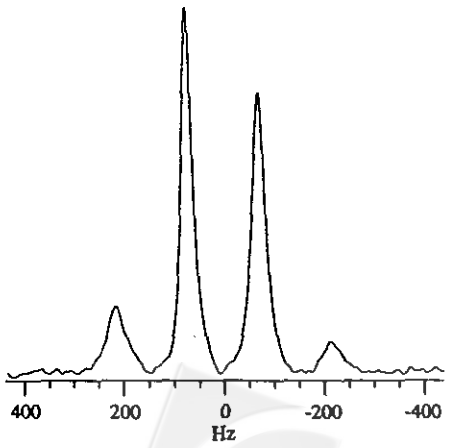

Fig. 5. Proton-coupled ^{13}C spectrum of the *N*-methyl group of CTAB at 75.5 MHz in a CTAB/Nasal viscoelastic micellar solution at 52 °C.

where $d_{q,0}^{(2)}(\beta)$ is the reduced Wigner rotation matrix element and where for the dipolar interaction of nucleus I and S, A_p is given by

$$A_2 = -D'I_+S_+$$
$$A_1 = -D'(I_ZS_+ + I_+S_Z)$$
$$A_0 = -(6)^{-1/2}D'(4I_ZS_Z - I_+S_- + -I_-S_+)$$
$$A_{-1} = A_1^*$$
$$A_{-2} = A_2^*$$

where S = 1/2 denotes the spin quantum number for one proton spin only, $D' = (3/2)^{1/2}\gamma_I\gamma_S\hbar/r^3$, where γ_I and γ_S are the gyromagnetic ratios of the I and S spins, respectively, and r is the C-H bond length.

In formulating the DLB we start from the stochastic Liouville equation and consider the overall orientation and internal rotation as independent motions,

$$\dot{\rho}(\Omega,\alpha,t) = \{-i(\hat{L}_Z + \hat{L}_{DD}) - \hat{\Gamma}_\Omega - \hat{\Gamma}_\alpha\}\rho(\Omega,\alpha,t) \quad (22)$$

where ρ is the spin density matrix in a state (Ω,α). Γ_α and Γ_Ω are the diffusion operators for internal rotation and overall reorientation, respectively. L_Z and L_{DD} are the Liouville operators corresponding to the Zeeman interactions (i.e., H_Z) and the dipolar interactions (i.e., H_{DD}) of the system, respectively. Since the internal rotational motion is considered a priori to be much faster than the overall reorientation, α characterizes the fast internal motion, which may be deemed to be independent of the overall reorientation. Thus, a coarse graining in time is introduced such that the spin density operator is averaged over a period of time much longer than the correlation time of the internal rotation but still small compared to the correlation time of overall reorientation. Following the approach of Hwang,[114] the SLE is then reduced by averaging over the fast variable and treating the dipolar interaction as a perturbation. This then gives,

$$\dot{\sigma}(\Omega,t) = [-i(\hat{L}'_Z + \hat{L}'_{DD}) - \hat{\Gamma}_\Omega - 1/T_2(\Omega)]\sigma(\Omega,t) \quad (23)$$

where the reduced density matrix σ is defined as the density matrix after isotropic averaging over α. L_{DD}' is the Liouville operator corresponding to the averaged dipolar Hamiltonian:

$$\mathcal{H}'_{DD} = \langle\mathcal{H}_{DD}(\Omega,\alpha)\rangle_\alpha = S_{C_3}d_{0,0}^{(2)}(\beta)\sum_p D_{0,p}^{(2)}(\Omega)A_p \quad (24)$$

S_{C_3} is the order parameter for the C_3 axis of the methyl group and is defined as

$$S_{C_3} = \frac{1}{2}\langle 3\cos^2\theta - 1\rangle_\alpha \quad (25)$$

where θ is the angle between the C_3 axis and the director of the aggregate. The averaging is over the fast intemal motion α. L_0' is the Liouville operator corresponding to the averaged $H_Z$in which the CSA interaction is averaged over α (i.e., averaged over the fast motion). Thus assuming that the correlation time for intemal reorientation is within the extreme narrowing condition, the internal molecular-orientation spin-spin relaxation rate, at the instant of molecular orientation specified by the Euler angle Ω, due to the modulation of the dipolar interaction by the internal rotation is given by

$$\frac{1}{T_2(\Omega)} = X + YD_{0,0}^{(2)}(\Omega) \quad (26)$$

where

$$X = N\gamma_C^2\gamma_H^2\hbar^2S(S+1)r^{-6}\cdot[2\sin^2(2\beta)\tau_1 + \sin^4(\beta)\tau_2] \quad \text{and} \quad (27)$$

$$Y = N\gamma_C^2\gamma_H^2\hbar^2S(S+1)r^{-6}\cdot[\sin^2(2\beta)\tau_1 - \sin^4(\beta)\tau_2]/4. \quad (28)$$

N = 3 denotes the number of methyl protons, γ_C and γ_H are the carbon and proton gyromagnetic ratios, respectively. τ_1, and τ_2 are the correlation times for intemal rotation with $\tau_2 = \tau_1/4$ for the Brownian model. The reduced stochastic equation may be solved by the eigen-function expansion method of Freed and co-workers.[115,116] The eight possible spin states of the three methyl protons can be separated into a quartet (S = 3/2) and two doublets (S = 1/2).[117] The proton-coupled ^{13}C spectrum is then treated as a superposition of individual spectra from the separate coupling of the ^{13}C with one S = 3/2 spin and two S = 1/2 spins. Further, the motionally narrowed results may be obtained by retaining the second order terms in the interactions. The perturbation method for solving the SLE is

known.[115,116,118,119] Similarly a modified motional narrowing line width equation for proton-coupled ^{13}C spectra may be derived. The equation includes the effects of CSA, DD and CSA-DD cross-interactions. If the overall reorientational diffusion is assumed to be isotropic and Brownian, the results may be expressed by the formula

$$1/T_2(m_s, \tau) = a + bm_s + cm_s^2 \quad (29)$$

where m_s is the magnetic spin quantum number of the protons with total spin quantum number defined by S. Here we limit ourselves to the square term of m, and neglect the higher m_s terms. The parameters a, b and c in units of rad s^{-1} are given by

$$a \equiv a' + X + \tau_0\left\{\frac{1}{5}S_{C_3}^2(F^2 - Y^2) + \frac{3}{20}S_{C_3}^2F^2U_0 + \frac{1}{5}S(S+1)D^2\left(P + \frac{1}{3}U_- + 2U_3\right)\right\} \quad (30)$$

$$b \equiv -\left(\frac{32}{75}\right)^{1/2}\tau_0 S_{C_3}FD\left(1 + \frac{3}{4}U_0\right) \quad (31)$$

$$c \equiv \frac{8}{15}\tau_0 D^2\left(1 - \frac{3}{8}P + \frac{3}{4}U_0 - \frac{1}{8}U_- - \frac{3}{4}U_+\right) \quad (32)$$

where τ_0 is the correlation time of the overall motion, $D \equiv S_{C_3}d_{0,0}^{(2)}(\beta)D'$ and a' is a residual linewidth which is considered to be attributable to spin-rotation interaction and other unspecified relaxation mechanisms such as long-range intramolecular or intermolecular DD relaxations. We also define

$$P \equiv (1 + (\omega_H\tau_0)^2)^{-1} \quad (33)$$

$$U_0 \equiv (1 + (\omega_C\tau_0)^2)^{-1} \quad (34)$$

$$U_\pm \equiv [1 + (\omega_C \pm \omega_H)^2(\tau_0)^2]^{-1} \quad (35)$$

where ω_C and ω_H are the ^{13}C and ^1H Larmor frequencies, respectively.

Since $^1J_{CH}$ is known to be positive the resonances from downfield to upfield (i.e., left to right) correspond to the m_s = 3/2, 1/2, -1/2 and -3/2 proton states. In addition to the cross-correlation effects the linewidths of the resonances are affected by sample temperature variation during spectral acquisition, magnetic field inhomogeneity, unresolved long range couplings and scalar relaxation due to the fast relaxing ^{14}N nucleus. However, in contrast to the cross-correlation effects, these other linebroadening mechanisms affect each of the multiplet resonances equally. Further these other mechanisms are cancelled since we use the difference in linewidth between the multiplets. At 52 °C the difference in linewidth between the linewidths (i.e., full width at half height) of the resonances of the resonances corresponding to m_s = -1/2 and 1/2 and m_s = 3/2 and 1/2 proton states are 4.6 ± 0.5 and 18.5 ± 1.5 Hz, respectively. The m_s-dependent terms (see b and c in Eq. (29)) can be directly deduced from these linewidth differences, while the m_s-independent terms cancel. It can be shown that,

$$\pi\Delta\nu\,(-1/2, 1/2) = 1/T_2(-1/2) - 1/T_2(1/2) = -b \quad (36)$$

$$\pi\Delta\nu\,(3/2, 1/2) = b + 2c \quad (37)$$

where the numbers in parentheses represent the proton spin states and $\Delta\nu$ denotes the difference in linewidth in Hertz. The b term arises from DD-CSA interference (Eq. (31)) whilst the c term arises only from DD relaxation (Eq. (32)). At 7.0 T and $\tau_0 \sim 10^{-8}$ s the spectral densities U_0, $U_\pm$ and P are negligibly small (~ 0.01). Since the dipolar interaction between the ^{13}C and the protons can easily be estimated, the determination of b and c gives direct information on the value of τ_0 and the chemical shift anisotropy. From the linewidth differences given above and assuming that the order parameter, S_{C_3} = 0.11, it was found that the correlation time for the overall reorientational motion (i.e., τ_0) = 1.8 ± 0.25 μs and $\Delta\sigma$ = -57 ± 7 ppm.

Example 2: The Hypophosphite Ion - A Probe of Erythrocyte Intracellular Viscosity

The cytoplasmic viscosity of erythrocytes can have broad physiological effects. Increased viscosity will reduce red cell deformability, which will ultimately affect blood circulation. Viscosity can also alter metabolic processes within the cell through its effect on the diffusion rate of substrate species involved in diffusion controlled reactions. Most methods of studying blood viscosity report only on the bulk properties of the blood. NMR provides a convenient and non-invasive means of specifically studying the intracellular viscosity. As an example we consider the hypophosphite ion, which forms an AX_2 spin system. HP is a particularly useful probe for erythrocyte studies since it is a structural analog of both the phosphate and bicarbonate ions and when placed in an erythrocyte suspension it rapidly transports into the cytoplasm via the anion transport protein, Band 3.[120] Its use as an NMR probe is facilitated by the intracellular and extracellular HP species appearing as separate resonances.

The Hamiltonian for this system may be defined as

$$\mathcal{H} \equiv \mathcal{H}_Z + \mathcal{H}_{CSA} + \mathcal{H}_{DD} + \mathcal{H}_{SR} \quad (38)$$

where the spin-rotation Hamiltonian is defined by,

$$\mathcal{H}_{SR}(t) = \hbar^{-1} \sum_{v=1}^{3} \sum_{m=-1}^{1} b'^{*}_{mv} I_v D^{1*}_{qm}(\Omega(t)) \omega_v(t) \quad (39)$$

where I_v (v = 1,2,3) are the principal moments of inertia, ω_v (v = 1,2,3) are the corresponding components of angular velocity; the Euler angle, $\Omega(t)$, specifies the orientation of the principal axis of the spin rotation tensor in the molecule to the laboratory frame, and we define,

$$b'_{ov} = C'_{3v}$$

$$b'_{\pm 1v} = \mp \frac{C'_{1v} \mp iC'_{2v}}{\sqrt{2}}$$

$$b'_{-mv} = (-)^m b'^{*}_{mv}$$

where C_{1v}', C_{2v}' and C_{3v}' are the components of the spin-rotation tensor.[38]

At lower magnetic field strengths the CSA term is small and so the effects of cross-correlation are correspondingly small (in comparison to the normal Zeeman relaxation). Hence to measure two-spin order relaxation we selectively excited two-spin order coherence using a variation of the DEPT pulse sequence,[121]

$$(\pi/2)^{H}_{x} - 1/(2J_{PH}) - (\pi/2)^{H}_{\phi} - t - (\pi/2)^{P}_{\phi} - Acq$$

where t is the evolution time and J_{PH} is the phosphorus to proton spin-spin coupling constant expressed in Hertz. The two proton pulses generate $^1H \rightarrow {}^{31}P$ coherence transfer and the phosphorus pulse converts two spin coherence into single-quantum coherence for ^{31}P observation. Immediately after the generation of coherence transfer the density matrix for the system is given by,[121]

$$\rho(t = 0) \simeq (1/8)(1 + \hbar\omega_P I_z/kT \pm \hbar\omega_H(2I_zS_z)/kT) \quad (40)$$

where ω_P and ω_H are the ^{31}P and ^1H Larmor frequencies, respectively. The sign of the third term depends on the phase (i.e., $\phi = \pm y$) of the second proton pulse.

Relaxation behavior in coupled spin systems is conveniently treated by using the normal-mode formalism.[42,122,123] Most normal modes can be obtained directly from the spectra as sums or differences of line intensities. Redfield theory[37,38] is used to calculate the relaxation processes including terms for cross-correlation,

$$\frac{dO}{dt} = -RO \quad (41)$$

where **R** is the Redfield relaxation matrix appropriate to the system (see below) and the array of spin operators **O** is defined as

$$\tilde{O} = [O_1, O_2, O_2, O_3, O_4, O_5, O_6, O_7] \quad (42)$$

where

$$\begin{aligned}
O_1 &\equiv S0(0) - I^0_z \equiv {}^{a}_{0}\nu_1^{AX_2} - I^0_z \equiv \langle I_z - I^0_z \rangle \equiv \langle \Delta I_z \rangle \\
O_2 &\equiv U1(1) - S^0_z/\sqrt{2} \equiv {}^{a}_{0}\nu_2^{AX_2} - S^0_z/\sqrt{2} \\
&\equiv \langle S_z - S^0_z \rangle/\sqrt{2} \equiv \langle \Delta S_z \rangle/\sqrt{2} \\
O_3 &\equiv S0(2) \equiv \frac{-1}{\sqrt{3}}\left({}^{a}_{0}\nu_3^{AX_2} + \sqrt{2}\, {}^{a}_{u}\nu_4^{AX_2} \right) \\
&\equiv -\left[4\langle I_zS'_zS''_z\rangle + 2\langle (S'_+S''_- + S'_-S''_+)I_z\rangle\right]/\sqrt{3} \\
O_4 &\equiv S2(2) \equiv \frac{1}{\sqrt{3}}\left(\sqrt{2}\, {}^{a}_{0}\nu_3^{AX_2} - {}^{a}_{0}\nu_4^{AX_2}\right) \\
&\equiv 2\left[4\langle I_zS'_zS''_z\rangle - \langle (S'_+S''_- + S'_-S''_+)I_z\rangle\right]/\sqrt{6} \\
O_5 &\equiv S1(1) \equiv {}^{s}_{0}\nu_1^{AX_2} \equiv \sqrt{2}\langle I_zS_z\rangle \\
O_6 &\equiv U0(2) \equiv \frac{-1}{\sqrt{3}}\left({}^{s}_{u}\nu_2^{AX_2} + \sqrt{2}\, {}^{s}_{u}\nu_3^{AX_2} \right) \\
&\equiv -\left[2\langle S'_zS''_z\rangle - \langle (S'_+S''_- + S'_-S''_+)\rangle\right]/\sqrt{6} \\
O_7 &\equiv U2(2) \equiv \frac{1}{\sqrt{3}}\left(\sqrt{2}\, {}^{s}_{u}\nu_2^{AX_2} - {}^{s}_{u}\nu_3^{AX_2}\right) \\
&\equiv \left[4\langle S'_zS''_z\rangle - \langle (S'_+S''_- + S'_-S''_+)\rangle\right]/(2/\sqrt{3})
\end{aligned}$$

where the U and S operators of Bain and Lynden-Bell[124] have been written in operator form. In the above expressions the operators **I** and **S** (≡ S′ + S″) denote the A and X spins, respectively and the superscript, *0*, represents the equilibrium value of the corresponding spin operators. The normal mode (*i.e.*, the terms ${}^{x}_{y}\nu_z^{AX_2}$; these terms are defined in Ref. 42) equivalents of the spin operators are also given.

R is given in the work of Bain and Lynden Bell[124] and includes terms for CSA and DD interactions. A completely asymmetric CSA tensor is built into the relaxation matrix as the sum of two axially symmetric CSA tensors. By analogy to the work of Goldman[38] the CSA terms of the A spin are replaced by the following equations:

$$(\sigma_{\parallel}^{A} - \sigma_{\perp}^{A})^2 \rightarrow (\sigma_x^A - \sigma_z^A)^2 + (\sigma_y^A - \sigma_z^A)^2 - (\sigma_x^A - \sigma_z^A)(\sigma_y^A - \sigma_z^A) \quad (43a)$$

$$(\sigma_{\parallel}^{A} - \sigma_{\perp}^{A})^2 P_2(\cos\delta) \rightarrow (\sigma_x^A - \sigma_z^A)^2 P_2(\cos\theta'_{xz}) + (\sigma_y^A - \sigma_z^A) P_2(\cos\theta'_{yz}) \quad (43b)$$

where P_l is the Legendre function, δ is the angle between the AX internuclear vector and the principal axis of the CSA tensor, and the angles $\theta_{xz'}$ and $\theta_{yz'}$ define the relative orientation between the IS internuclear vector (i.e., z' directed along P-H) with respect to the principal axes x and y of the chemical shift shielding tensor of HP, σ.

The observed intensities of proton-coupled ^{31}P triplet resonances at $\omega_P + J_{PH}, \omega_P, \omega_P - J_{PH}$ are proportional to

$$O_1/4 - O_3/(4\sqrt{3}) + O_4/(2\sqrt{6}) - O_5/(2\sqrt{2}) \quad (44a)$$

$$O_1/2 + O_3/(2\sqrt{3}) - O_4/\sqrt{6} \quad (44b)$$

$$O_1/4 - O_3/(4\sqrt{3}) + O_4/(2\sqrt{6}) + O_5/(2\sqrt{2}), \quad (44c)$$

respectively. The linear combinations of the resonance intensities of the proton-coupled ^{31}P triplet in the inversion recovery experiments give rise to the observed $<2I_zS_z(t)>$ (i.e., Eqs. (44a)-(44c)) and $<I_zS_z'S_z''(t)>$ (i.e., Eqs. (44b)-(44a)-(44c)). By considering Eq. (44) and comparing the sign of $<2I_zS_z(t)>$ and $<I_zS_z'S_z''(t)>$ obtained from the inversion recovery experiment where both the ^{31}P and ^{1}H spins are inverted, the sign of the spin-spin coupling constant (i.e., J_{PH}) can be determined. An alternative method is to observe the relative relaxation of the proton-coupled ^{31}P triplet.

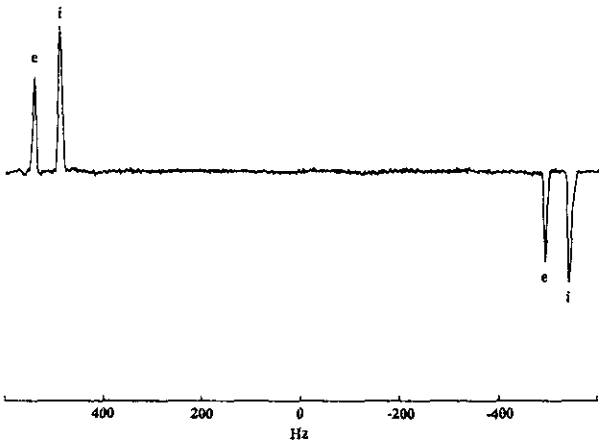

Fig. 6. ^{31}P $2I_zS_z$ spectrum of HP (0.8 M) in a suspension erythrocytes at 310 K and 121.4 MHz. The suspending solution was hypertonic so that the average erythrocyte volume was 56 fl. The erythrocyte suspension has a hematocrit of 91%. The spectrum appears as a pair of antiphase doublets from the intracellular (i) and extracellular (e) species, respectively. Compared to the intracellular resonance the extracellular resonance is small due to the high hematocrit. The difference in absolute intensity between the resonances of the doublet resulting from the intracellular HP is due to the effects of CSA-DD cross-interactions.

^{31}P difference spectra, recorded for each value of the evolution time, appear as antiphase doublets of spectral resonances. A difference spectrum of HP in an erythrocyte suspension is given in Fig. 6. The difference in intensity of the two (antiphase) resonances is related to the evolution of the $<I_zS_z>$ terms. The time evolution of $<\Delta I_z(t)>$ is calculated from Eq. (41) with the initial expectation values of the multispin operators (defined in Eq. (42)). The initial expectation values of the multispin operators are calculated from the initial density matrix given in Eq. (39) and the equilibrium distribution. We obtain $<\Delta I_z(0)> = 0$, $<\Delta S_z(0)> = -\hbar\omega_H/2kT$, $<\Delta I_zS_z(0)> = \pm \hbar\omega_H/8kT$ and the expectation values of the other multispin operators vanish. The experimental and calculated results are expressed in terms of $<\Delta I_zS_z(t))/I_z^0$, where the superscript 0 denotes the equilibrium value. In practice the equilibrium value is obtained from the spectral resonance acquired using only a very short evolution time (e.g., 1 ms). A plot of the $<2I_zS_z>$ time evolution in D_2O solutions at various temperatures is given in Fig. 7. The orientation of the HP

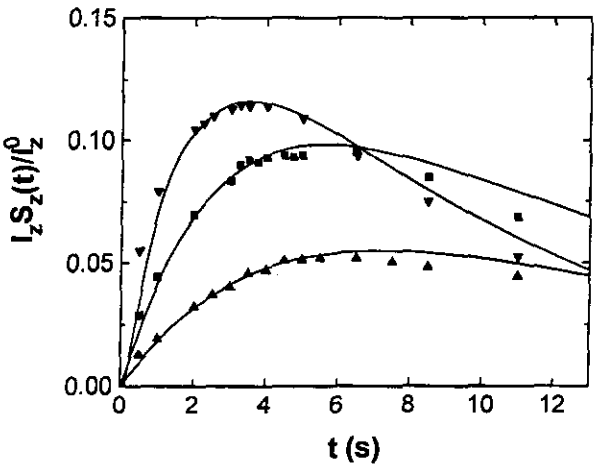

Fig. 7. $2I_zS_z$ relaxation profiles for HP (1 M) in D_2O at 276 K (▼), 294 K (■) and 329 K (▲). The ^{31}P NMR measurements were performed at 121.4 MHz. The results were simulated (represented by solid lines) without including terms for random field relaxation.

chemical shift tensor to the molecular axis was determined by simulating the data (i.e., the solid lines in Fig. 7). A schematic representation of the orientation relative to the molecular axis is given in Fig. 8. τ_c is closely related to the locus of the maximum point of the two-spin order relaxation curve and thus the value of τ_c is readily determined from simulating the two-spin order data. The values of τ_c determined for HP in the D_2O solution at various temperatures is given in the caption to Fig. 7. Plots of $<2I_zS_z>$ time evolution of intracellular HP in erythrocyte suspensions of various cell volumes are given in Fig. 9. The cell volumes were adjusted by suspending the cells in buffers of different osmolalities. The values of τ_c determined for the intracellular HP in each cell sample are given in the figure caption. The effects of random field interactions are determined from the degree of depression of the intensity of the $<2I_zS_z>$ relaxation profile. Since the random field interactions are small, the locus of the maximum point (i.e., the evolution time) decreases with increasing viscosity and therefore τ_c. The solution viscosity may then be inferred from this correlation time and the molecular dimensions of HP. The simplest means of relating τ_c to solution viscosity is by the Debye equation.[125,126] However, in the present example a basic assumption of the Debye theory is violated since the physically small HP cannot 'see' the solvent (mainly hemoglobin and H_2O) as a continuum. Examples of modifications to the Debye equation to take into account the discontinuous nature of the solvent and for nonsphericity of the probe molecule may be found elsewhere.[126]

DLB effects are not observable in spectra of HP in erythrocyte cytoplasm unless the cells have been shrunk by suspension in very hypotonic solutions. If HP is dissolved in a concentrated albumin solution, however, DLB is readily observed (see Fig. 10). The effect becomes more pronounced at longer reorientational correlation times (i.e., at higher albumin concentrations and lower temperatures). DLB has also been observed for HP in lysozyme solution.[55]

CONCLUSIONS

Apart from the obvious gains in signal-to-noise ratios, all of the three techniques discussed in this review will benefit from the availability of increasingly higher static magnetic field strengths. The null point method will benefit since the bound quadrupolar nuclei are more likely to be outside the extreme narrowing condition. Whereas CSA-DD cross-correlation is directly proportional to the static magnetic field strength. Even if the CSA spectral density is small, the coupling of it with the DD spectral den-

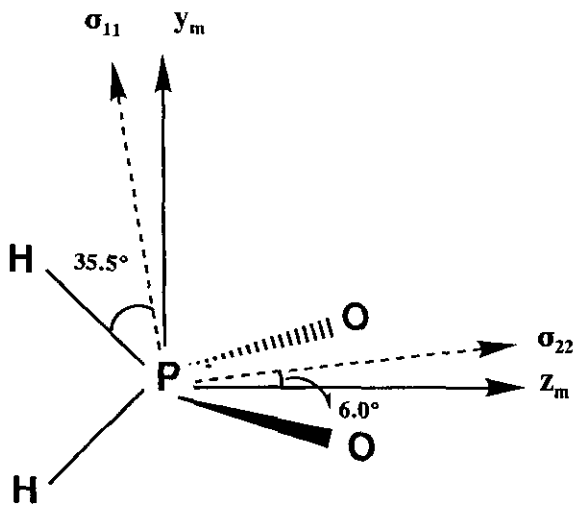

Fig. 8. Schematic diagram of the hypophosphite ion showing the relative orientation of the chemical shift tensor with respect to the molecular frame. The molecular frame is denoted by the subscript m. There is a 6 tilt angle between the σ_{22} direction and the O-P-O plane (i.e., θ_{yz} = 35.5°). σ_{33} and x_m are perpendicular to the axes shown and are directed out of the page.

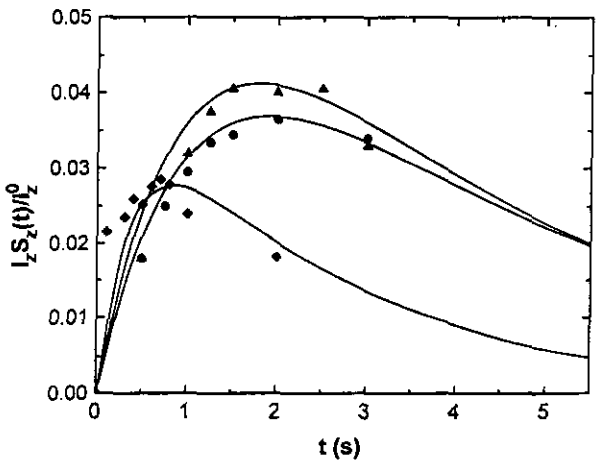

Fig. 9. $2I_zS_z$ relaxation profiles for HP (0.8 M) in erythrocytes suspensions at 310 K. The ^{31}P NMR measurements were performed at 121.4 MHz. The relaxation data (symbols) and simulated relaxation profiles (lines) are for 56 (♦), 69 (▲) and 85 fl (•) cells. The correlation times determined for the different cell suspensions in order of increasing cell size were 15.2, 10.6, and 7.9 ps.

sity may make it significant.[69,127] Dalvitt[80] has remarked that for ice the proton chemical shift anisotropy (i.e., $\Delta\sigma$) is 34 ppm[128] and at 600 MHz this corresponds to an interaction of 20.4 kHz and thus CSA-DD cross-interactions may contribute to the observed ^1H relaxation of water at high fields.

This review has shown that the null point method while being an experimentally simple is capable of providing more information than traditional (i.e., T_1 and T_2) measurements. It allows more accurate estimates of correlation times to be determined and the shape of the null point can be used to infer order properties of ion binding sites. Of major significance is that this method obviates the need for (unreliable) multiexponential regressions onto relaxation data. This feature opens the way for studying quadrupolar nuclei with higher spin quantum numbers and experiments in this laboratory are currently in progress. The null point method also provides a convenient means to observe the dynamic frequency shift. Although the relevant spin dynamics and quadrupolar relaxation mechanism can be handled using standard density matrix formalism, the use of state multipoles allows intuitive insight into the relaxation processes occurring in addition to simplifying the necessary calculations.

The effects of cross-correlation should continue to increase in their use and application in the literature. It is also envisaged that with higher static field strengths the prevalence of 'anomalous cross-peaks' in two-dimensional spectra will increase. Of particular significance to solution state studies is that the CSA-DD cross-interaction, which is very common in biological spin-systems, can be used to separate random field interactions thereby allowing more accurate estimates of the reorientational correlation times. Further, the CSA-DD cross-interaction can be used to determine motional anisotropy. The application of differential line broadening to the study of membrane bound molecules should also increase.

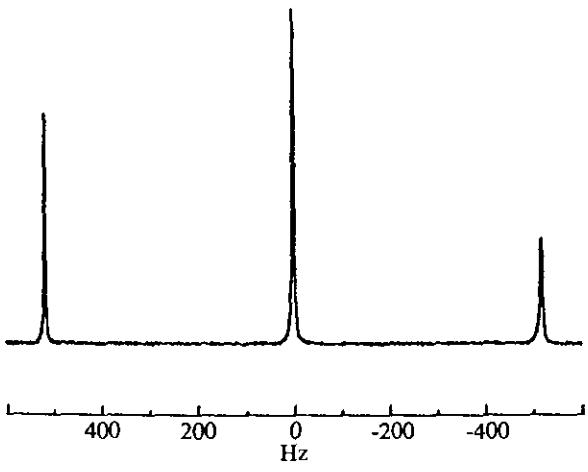

Fig. 10. Differential line-broadening of the proton-coupled ^{31}P spectrum of HP (0.8 M; pH 7.4) in bovine serum albumin (0.1 g ml^{-1}) at 121.4 MHz and 280 K. The effects of differential line-broadening are clearly shown by the difference in intensity of the satellite peaks. The linewidths (from left to right) are 2.0, 3.3 and 5.5 Hz, respectively.

ACKNOWLEDGMENT

Support of this work by grants from the National Science Council of the Republic of China is gratefully acknowledged.

Received September 1, 1992.

Key Words

NMR; Cross-correlation; Cross-interaction; Interference; Null point; Two-spin order; Three-spin order.

REFERENCES

1. Hubbard, P. S. J. *Chem. Phys.* **1970**, *53*, 985.
2. Bull, T. E. *J. Magn. Reson.* **1972**, *8*, 344.
3. Springer, C. S. Jr. *Ann. Rev. Biophys. Biophys. Chem.* **1987**, *16*, 375.
4. Fatemi, S. J. A.; Kadir, F. H. A.; Moore, G. R. *Biochem. J.* **1991**, *280*, 527.
5. Birchall, J. D.; Chappell, J. S. *Chin. Chem.* **1988**, *34*, 265.
6. Ge, N. H.; Price, W. S.; Hong, L. Z.; Hwang, L. P. *J. Magn. Reson.* **1992**, *97*, 656.
7. Price, W. S.; Ge, N. H.; Hong, L. Z.; Hwang, L. P. *J. Am. Chem. Soc.* submitted to publications.
8. Price, W. S.; Kuchel, P. W.; Cornell, B. A. *Biophys. Chem.* **1991**, *40*, 329.
9. Minami, T.; Price, W. S.; Cutler, D. J. *J. Pharm . Sci.* **1992**, *81*, 419.
10. Lindman, B.; Forsén, S. *Chlorine, Bromine and Iodine NMR. Physico-chemical and Biological Applications. NMR Basic Properties and Progress;* Diehl, P.; Fluck, E.; Kosfeldt, R. Eds.; Springer Verlag: Berlin, **1976**; Vol. 12.
11. Forsén, S.; Lindman, B. *Chem. Brit.* **1982**, *14*, 29.
12. Forsén, S.; Lindman, B. *Ion Binding in Biological Systems Measured by Nuclear Magnetic Resonance.* In

Methods of Biological Analysis; Glick, D. Ed.; Wiley: New York, **1981**; Vol. 27.
13. Forsén, S.; Drakenberg, T.; Wennerström, H. *Quart. Rev. Biophys.* **1987**, *19,* 83.
14. Bull, T. E. *J. Chem. Phys.* **1979**, *70,* 3106.
15. Reuben, J.; Luz, Z. *J. Chem. Phys.* **1976**, *80,* 1357.
16. Chung, W. W.; Wimperis, S. *Mol. Phys.* **1992**, *76,* 47 and pertinent references therein.
17. Rooney, W. D.; Springer, C. S. Jr. *NMR in Biomedicine* **1991**, *4,* 209.
18. Rooney, W. D.; Springer, C. S. Jr. *NMR in Biomedicine* **1991**, *4,* 227.
19. Eliav, U., Shinar, H.; Navon, G. *J. Magn. Reson.* **1992**, *98,* 223 and pertinent references therein.
20. Price, W. S.; Ge, N. H.; Hwang, L. P. *J. Magn. Reson.* **1992**, *98,* 134.
21. Haslinger, E.; Lynden-Bell, R. M. *J. Magn. Reson.* **1978**, *31,* 33.
22. Haslinger, E.; Robien, W. *J. Am. Chem. Soc.* **1980**, *102,* 1237.
23. Haslinger, E.; Robien, W.; Schölm, R. *J. Organomet. Chem.* **1980**, *194,* 331.
24. Haslinger, E.; Kalchhauser, H.; Robien, W. *J. Mol. Liq.* **1984**, *28,* 223.
25. Lee, T. S.; Hwang, L. P. *J. Magn. Reson.* **1990**, *89,* 51.
26. Urry, D. W.; Trapane, T. L.; Brown, R. A.; Venkatachalam, C. M.; Prasad, K. U. *J. Magn. Reson.* **1985**, *65,* 43.
27. Urry, D. W.; Trapane, T. L.; Venkatachalam, C. M.; Prasad, K. U. *J. Am. Chem. Soc.* **1986**, *108,* 1448.
28. Sanctuary, B. C. *J. Magn. Reson.* **1985**, *61,* 116 and pertinent references therein.
29. Werbelow, L. G. *J. Magn. Reson.* **1983**, *52,* 282.
30. Sanctuary, B. C., Halstead, T. K. *Bull. Magn. Reson.* **1989**, *11,* 32.
31. Rose, M. E. *Elementary Theory of Angular Momentum;* Wiley: New York, **1957**.
32. Brink, D. M.; Satchler, G. R. *Angular Momentum;* University Press: Oxford, **1968**.
33. Furó, I; Halle, B.; Wong, T. C. *J. Chem. Phys.* **1988**, *89,* 5382.
34. Cohen, M. H.; Reif, E. *Solid State Phys.* **1957**, *5,* 321.
35. Abragam, A. *The Principles of Nuclear Magnetism;* Clarendon Press: Oxford, **1961**.
36. Halle, B.; Wennerstrom, H. *J. Chem. Phys.* **1981**, *75,* 1928.
37. Redfield, A. G. In *Advances in Magnetic Resonance;* Waugh, J. S., Ed.; Academic Press: San Diego, **1965**; Vol. 1; pp 1-32.
38. McConnell, J. *The Theory of Nuclear Magnetic Relaxation in Liquids;* Cambridge University Press: Cambridge, **1987**.
39. Krishnan, V. V.; Kumar, A. *J. Magn. Reson.* **1991**, *92,* 293.
40. Petit, D.; Korb, J.-P.; Delville, A.; Grandjean, J.; Lazlo, P. *J. Magn. Reson.* **1992**, *96,* 252.
41. Vold, R. L.; Vold, R. G. Prog. *NMR Spectr.* **1978**, *12,* 79.
42. Werbelow, L. G.; Grant, D. M. *Adv. Magn. Reson.* **1977**, *9,* 189.
43. Canet, D. *Prog. NMR Spec.* **1989**, *21,* 237.
44. Canet, D.; Robert, J. B. *NMR Basic Principles and Progress,* **1990**; Vol. 25. pp 45-89.
45. Grant, D. M.; Mayne, C. L.; Liu, F.; Xiang, T. X. *Chem. Rev.* **1991**, *91,* 1591.
46. Withers, S.; Madsen, N.; Sykes, B. *J. Magn. Reson.* **1985**, *61,* 545.
47. Werbelow, L. G. *J. Magn. Reson.* **1987**, *71,* 151.
48. Wang, P. L.; Hwang, L. P. *J. Phys. Chem.* **1988**, *92,* 623.
49. Hwang, L. P.; Wang, P. L.; Wong, T. C. *J. Phys. Chem.* **1988**, *92,* 4753.
50. Wong, T. C.; Wang, P. L.; Duh, D. M.; Hwang, L. P. *J. Phys. Chem.* **1989**, *93,* 1295. The b term in Eq. (24) in this reference should be defined negatively.
51. Chang, W. T.; Hwang, L. P.; Wang, P. L. *J. Chin. Chem. Soc.* **1989**, *36,* 417.
52. Chang, W. T.; Wang, P. L.; Duh, D. M.; Hwang, L. P. *J. Phys. Chem.* **1990**, *94,* 1343.
53. Chang, C. F.; Hwang, L. P. *J. Chin. Chem. Soc.* **1991**, *38,* 1.
54. Tsai, C. L.; Price, W. S.; Chang, Y. C.; Pemg, B. C.; Hwang, L. P. *J. Phys. Chem.* **1991**, *95,* 7546.
55. Price, W. S.; Perng, B. C.; Tsai, C. L.; Hwang, L. P. *Biophys. J.* **1992**, *61,* 621.
56. Königsberger, E.; Sterk, H. *J. Chem. Phys.* **1985**, *83,* 2723.
57. Farrar, T. C.; Adams, B. R.; Grey, G. C.; Quintero-Arcaya, R. A.; Zuo, Q. *J. Am. Chem. Soc.* **1986**, *108,* 8190.
58. Goldman, M. *J. Magn. Reson.* **1984**, *60,* 437.
59. Jaccard, G.; Wimperis, S.; Bodenhausen, G. *Chem. Phys. Lett.* **1987**, *138,* 601.
60. Kontaxis, G.; Müller, N.; Sterk, H. *J. Magn. Reson.* **1991**, *92,* 332.
61. Brüschweiler, R.; Griesinger, C.; Emst, R. R. *J. Am. Chem. Soc.* **1989**, *111,* 8034.
62. Dalvit, C.; Bodenhausen, G., *Adv. Magn. Reson.* **1990**, *14,* 1.
63. Zuiderweg, E. R. P. *J. Magn. Reson.* **1987**, *71,* 283.
64. Peng, J. W.; Wagner, G. *J. Magn. Reson.* **1992**, *98,* 308.
65. Farrar, T. C.; Jablonsky, M. J. *J. Phys. Chem.* **1991**, *95,*

9159.
66. Hartzell, C. J.; Stein, P. C.; Lynch, T. J.; Werbelow, L. G.; Earl, W. L. *J. Am. Chem. Soc.* **1989**, *111*, 5114.
67. Bull, T. E. *J. Magn. Reson.*, **1987**, *72*, 397.
68. Dalvit, C.; Bodenhausen, G. *J. Am. Chem. Soc.* **1988**, *110*, 7924.
69. Dalvit, C.; Bodenhausen, G. *Chem. Phys. Lett.* **1989**, *161*, 554.
70. Werbelow, L. G. *J. Magn. Reson.* **1979**, *34*, 439.
71. Thevand, A.; Werbelow, L. *J. Magn. Reson.* **1992**, *97*, 192.
72. Mäer, L.; Kowalewski, *J. Chem. Phys. Lett.* **1992**, *192*, 595.
73. Burghardt, I.; Konrat, R.; Boclenhausen, G. *Mol. Phys.* **1992**, *75*, 467.
74. Bull, T. E. *J. Magn. Reson.* **1988**, *80*, 470.
75. McConnell, H. M. *J. Chem. Phys.* **1956**, *25*, 709.
76. Mackor, E. L.; MacLean, C. *Prog. NMR Spectrosc.* **1967**, *3*, 129.
77. Farrar, T. C.; Quintero-Arcaya, R. A. *Chem. Phys, Lett.* **1985**, *122*, 41.
78. Rueterjans, K.; Kaun, E.; Hull, W. E.; Limbach, H. H. *Nucleic Acids Res.* **1982**, *10*, 7027.
79. Gueron, M.; Leroy, J. L.; Griffery, R. H. *J. Am. Chem. Soc.* **1984**, *105*, 7262.
80. Dalvitt, C. *J. Magn. Reson.* **1992**, *97*, 645.
81. Lunsford, J. H.; Rothwell, W. P.; Shen, W. J. *J. Am. Chem. Soc.* **1985**, *107*, 1540.
82. Anet, F. A. L. *J. Am. Chem. Soc.* **1986**, *108*, 7102.
83. Macura, S.; Brown, L. R. *J. Magn. Reson.* **1985**, *62*, 328.
84. Shimuzu, H. *J. Chem. Phys.* **1964**, *40*, 3357.
85. Mackor, E. L.; MacLean, C. *J. Chem. Phys.* **1966**, *44*, 64.
86. Farrar, T. C.; Quintero-Arcaya, R. A. *J. Phys. Chem.* **1987**, *91*, 3224.
87. Harris, R. K.; Packer, K. J.; Thayer, A. M. *J. Magn. Reson.* **1985**, *62*, 284.
88. Oldfield, E.; Adebodun, F.; Chung, J.; Monetz, B.; Park, K. D.; Le, H. B.; Philips, B. *Biochemistry* **1991**, *30*, 11025.
89. Oldfield, E.; Chung, J.; Le, H. B.; Bowers, T.; Patterson, J.; Turner, G. L. *Macromol.* **1992**, *25*, 3027.
90. Gracz, H.; Agris, P., private communication.
91. Wong, T. C.; Thalberg, K.; Lindman, B.; Gracz H. *J. Phys. Chem.* **1991**, *95*, 8850.
92. Müller, N.; Bodenhausen, G.; Wuthrich, K.; Ernst, R. R. *J. Magn. Reson.* **1985**, *65*, 531.
93. Müller, N.; Ernst, R. R.; Wuthrich, K. *J. Am. Chem. Soc.* **1986**, *108*, 6482.
94. Müller, N.; Bodenhausen, G.; Ernst, R. R. *J. Magn. Reson.* **1987**, *75*, 297.
95. Rance, M.; Wright, P. E. *Chem. Phys. Lett.* **1986**, *124*, 572.
96. Wimperis, S.; Bodenhausen, G. *Chem. Phys. Lett.* **1987**, *140*, 41.
97. Wimperis, S.; Bodenhausen, G. *Mol. Phys.* **1989**, *66*, 897.
98. Bodenhausen, G. *Some Aspects of Multiple-Quantum NMR in Multinuclear Magnetic Resonance in Liquids and Solids - Chemical Applications;* Grainger, P.; Harris, R. K. Eds.; Kluwer Academic Publishers: Dordrecht, 1990; pp 147-155.
99. Kay, L. E.; Prestegard, J. H. *J. Am. Chem. Soc.* **1987**, *109*, 3829.
100. Braunschweiler, L.; Bodenhausen, G.; Ernst, R. R. *Mol. Phys.* **1983**, *48*, 535.
101. Emst, R. R.; Bodenhausen, G.; Wokaun, A. *Principles of NMR in One and Two Dimensions,* Oxford University Press: Oxford, **1987**.
102. Jaccard, G.; Wim,reris, S.; Bodenhausen, G. *J. Chem. Phys.* **1986**, *85*, 6282.
103. Brondeau, J.; Canet, D.; Millot, C.; Nevy, H.; Werbelow, L. G. *J. Chem. Phys.* **1985**, *82*, 2212.
104. Böhlen, J. M.; Wimperis, S.; Bodenhausen, G. *J. Magn. Reson.* **1988**, *77*, 589.
105. Keeler, J.; Sanchez-Ferrando, F. *J. Magn. Reson.* **1987**, *75*, 96.
106. Kay, L. E.; Torchia, D. A. *J. Magn. Reson.* **1991**, *95*, 536.
107. Di Bari, L.; Kowalewski, J.; Bodenhausen, G. *J. Chem. Phys.* **1990**, *93*, 7698.
108. Palmer, A. G.; Skelton, N. J.; Chazin, W. J.; Wright, P. E.; Rance, M. *Mol. Phys.* **1992**, *75*, 699.
109. Kay, L. E.; Nicholson, L. K.; Delaglio, F.; Bax, A.; Torchia, D. A. *J. Magn. Reson.* **1992**, *97*, 359.
110. Boyd, J.; Hommel, U.; Campbell, I. D. *Chem. Phys. Lett.* **1990**, *175*, 477.
111. Wennerström, H.; Lindman, B.; Soderman, O.; Drakenberg, T.; Rosenholm, J. B. *J. Am. Chem. Soc.* **1979**, *101*, 6860.
112. Lipari, G.; Szabo, A. *J. Am. Chem. Soc.* **1982**, *104*, 4546.
113. Lipari, G.; Szabo, A. *J. Am. Chem. Soc.* **1982**, *104*, 4559.
114. Hwang, L. P. *Mol. Phys.* **1983**, *49*, 1314.
115. Freed, J. H.; Bruno, G. V.; Polnaszek, C. F. *J. Phys. Chem.* **1971**, *75*, 3385.
116. Polnaszek, C. F.; Bruno, G. V.; Freed, J. H. *J. Chem. Phys.* **1973**, *58*, 3185.
117. Carrington, A.; McLachlan, A. D. *Introduction to Magnetic Resonance.* Harprer and Row: New York. **1967**; Chapter 4.
118. Freed, J. H. *J. Phys. Chem.* **1974**, *78*, 1155.

119. Hwang, J. S.; Mason, R. P.; Hwang, L. P.; Freed, J. H. *J. Phys. Chem.* **1975**, *79*, 489.
120. Price, W. S.; Kuchel, P. W. *NMR in Biomedicine* **1989**, *3*, 59.
121. Bulsing, J. M.; Doddrell, D. M. *J. Magn. Reson.* **1985**, *61*, 197.
122. Werbelow, L. G.; Marshall, A. G. *Mol. Phys.* **1974**, *28*, 113.
123. Werbelow, L. G.; Grant, D. M. *J. Magn. Reson.* **1975**, *20*, 554.
124. Bain, A. D.; Lynden-Bell, R. M. *Mol. Phys.* **1975**, *2*, 325.
125. Bloembergen, N.; Purcell, E, M.; Pound, R. V. *Phys. Rev.* **1948**, *73*, 679.
126. Boeré, R. T.; Kidd, R. G. *Ann. Rep. NMR Spectrosc.* **1982**, *13*, 319.
127. Werbelow, L. G. *J. Phys. Chem.* **1990**, *94*, 6663.
128. Pines, A.; Ruben, D. J.; Vega, S.; Mehring, M. *Phys. Rev. Lett.* **1976**, *36*, 110.